J. Membrane Biol. 25, 183–208 (1975)

Analog Circuit of the *Acetabularia* Membrane

D. Gradmann

Institut für Biologie I, Abteilung Biophysik, D-7400 Tübingen,
Auf der Morgenstelle 1, Germany

Received 15 May 1975; revised 14 July 1975

Summary. The high membrane potential of *Acetabularia* ($E_m = -170$ mV) is due to an electrogenic pump in parallel with the passive diffusion system ($E_d = -80$ mV) which could be studied separately in the cold, when the pump is blocked. Electrical measurements under normal conditions show that the pump pathway consists of its electromotive force E_P with two elements P_1 and P_2 in series; P_2 is shunted by a large capacitance ($C_P = 3$ mF cm^{-2}). The nonlinear current-voltage relationship of P_1 (light- and temperature-sensitive) could be determined separately; it reflects the properties of a carrier-mediated electrogenic pump. The value of E_P (-190 mV) indicates a stoichiometry of 2:1 between electrogenically transported charges and ATP. The electrical energy, normally stored in C_P, compares well with the metabolic energy, stored in the ATP pool. The nonlinear current-voltage relationship of P_2 (attributed to phosphorylating reactions) is also sensitive to light and temperature and is responsible for the region of negative conductance of the overall current-voltage relationship. The power of the pump (1 μW cm^{-2}) amounts to some percent of the total energy turnover. The high Cl^- fluxes (1 nmol cm^{-2} sec^{-1}) and the electrical properties of the plasmalemma are not as closely related as assumed previously. For kinetic reasons, a direct and specific Cl^- pathway between the vacuole and outside is postulated to exist.

During the past ten years, the emphasis in membrane biology has shifted from pure diffusion processes to active transport mechanisms. Numerous studies focus on the chemiosmotic hypothesis of Mitchell [23], worked out for the energy conserving mitochondrial membrane. The question arises, whether these mechanisms have universal significance for biomembranes. In fact, so-called electrogenic pumps are demonstrated in a wide variety of animal, fungal and plant cell membranes. These electrogenic pumps can be understood as the same device as ATP synthesis, driven by an electrical gradient across the membrane, only operating in the opposite direction, thus generating a voltage by ATP hydrolysis. Since electrophysiological studies on membranes of mitochondria, chloroplasts and bacteria rely on indirect methods, the detailed electrical properties of these membrane-bound ATPase systems should be investigated in objects accessible to microelectrode techniques.

Single cells of the giant marine green alga *Acetabularia* seem to be a favorable system. Previous studies have demonstrated that these cells exhibit an obvious electrogenic pump under normal conditions: Cl^- is probably the ion which is pumped in electrogenically by ATP hydrolysis [11, 26]. However, most of the published electrical data have only qualitative validity. The former current-voltage data of Gradmann [11] were only input measurements, neglecting the cable properties. Saddler's [27] data of the membrane resistance are also of limited significance, since the techniques and analysis of these experiments, worked out for *Nitella* [18], do not apply for *Acetabularia* where the length constant can be much shorter than the length of the cell. In order to incorporate the electrical properties in the total picture of the membrane, quantitative data are necessary. The first correct calculations about the linear cable properties of the *Acetabularia* membrane have been carried out recently [15], including some valid extensions to nonlinear current-voltage ranges.

New flux data [10] reveal many more details than did previous work [25]. Since it is possible now to measure electrical properties and ion fluxes simultaneously on individual cells of *Acetabularia* [16], considerable progress is expected in studying the correlation between these two types of measurements. In addition, ATP measurements are available now for some experimental conditions [14]. So it is possible to compare the energetics of the electrical membrane parameters with the energy metabolism of the cell.

On these experimental grounds (electrical data, flux measurements and ATP results) it seems to be possible to draw a consistent picture of the *Acetabularia* membrane. Though many details have to be worked out in further studies, it is the aim of this paper to give the framework of a quantitative model of the electrical properties of the *Acetabularia* membrane, including ion fluxes and energetics. Part of the data presented here were reported briefly at the 1974 *Acetabularia* Symposium in Paris [14] and in the abstracts of the meeting of the Deutsche Botanische Gesellschaft (1974) in Würzburg [12].

Materials and Methods

Material

Cells of *Acetabularia mediterranea* have been cultured in Erdschreiber solution, according to Hämmerling [17] and Beth [4]. For experiments, young cells have been used without a cap. The length varied from 2–4 cm, the diameter from 0.3–0.5 mm. These cells are long enough to provide the advantages of a giant cell. The approximately cylindrical shape favors

the analysis of the parameters related to the membrane area; furthermore, these growing cells have an active metabolism and on the apical end a tender cell wall, which facilitates puncture with microelectrodes. Occasionally, cells in different developmental states have been used; the difference in the membrane parameters between these cells is statistically insignificant.

General Conditions

The normal illumination of the cells mounted for measurements was about 0.1 mW cm^{-2} diffuse white light. This is mostly referred to darkness D in contrast to bright illumination L (100 mW cm^{-2}), by a spotlight from a quartz iodide lamp. The normal ambient temperature was about 23 ± 2 °C. A KG filter (Schott) prevented heating of the medium by irradiation from the light source. Low temperature experiments have been performed in a cold room or by cooling the measuring chamber with a thermostated fluid circuit. The outer medium was artificial seawater containing the following ions (in mM): Na^+ 461, K^+ 10, Mg^{++} 53, Ca^{++} 10, Cl^- 529, SO_4^{--} 28, HCO_3^- 2, usually buffered with 10 mM Tris-HCl at pH 8.0.

Electrical Measurements

The basic setup has been the same as described previously [11]. Briefly, standard microelectrode techniques have been applied. Voltages between the cell interior, probably the cytoplasm [15] and the outer medium have been measured by high impedance ($10^{12}\ \Omega$) difference amplifiers, the output of which was connected with a storage oscilloscope and a pen chart recorder.

In resistance measurements, current has been injected by a separate microelectrode and has been monitored to ensure the correct time course. With two voltage-recording electrodes at different distances from the current-injecting electrode, membrane resistance, capacity and the resistivity of the cell interior could be calculated according to the theory for finite and infinite cables [19].

The voltage-clamp circuit has been described earlier [11]. Point-clamp experiments with two electrodes (I_0 and V_0) have been analyzed by Cole's theorem [6]. In cases beyond the validity of this method (negative conductance and finite cable length) the technique of Adrian, Chandler and Hodgkin [1] has been used, with two voltage-recording electrodes close to one end (the apical one in our case) of the cell, where the difference between the recorded voltages (here smaller than 10 mV) is proportional to the membrane current; the current electrode was also placed close to the cell end. The scaling factor for the membrane current has been determined by referring the values for small voltage displacements to the average resistance data obtained by linear cable theory, rather than calculating this factor from the exact location of the electrodes in the cell.

Flux Measurements

As tracers for Cl^- and K^+ fluxes $^{36}Cl^-$ and $^{86}Rb^+$ have been used. Incubation medium was artificial seawater. For influx measurements, samples have been taken at different times after beginning of incubation. After short rinsing in cold medium, the uptake of radioactivity has been determined in a liquid scintillation counter after addition of scintillation gel. For efflux experiments, in most cases completely loaded cells have been mounted in an open vessel and washed with nonradioactive medium which has been sampled in short intervals (5–600 sec). The released radioactivity has been measured again in the liquid scintillation counter. The data have been analyzed basically according to Cram [7].

ATP Experiments

ATP concentrations have been determined according to Strehler [32]. Samples of about 15 cells have been killed in petroleum ether cooled at 173–183 °K by fluid nitrogen. After freeze-drying for about 20 hr, the cells have been cleaned from external salt crystals and weighed; 1 cell yielded about 0.5 mg. At 0 °C the samples have been extracted in 6% $HClO_4$ solution for 30 min. One sample, used for inner standard, contained additional ATP (50 ng ml^{-1}). The neutralized extracts have been put in front of a photomultiplier in the dark, where an aliquot of firefly extract (Sigma) could be injected (Skan Bioluminescence measuring device XP 2000). The resulting voltage peak could be recorded as a measure of the ATP concentration and compared with a calibration curve.

In order to measure the ATP turnover (compare [30, 31]), cells have been suddenly exposed to a high concentration of CCCP (50 μM) for different intervals and then abruptly frozen for fixation and ATP determination. The ATP decay during the first seconds after exposure to CCCP can be fitted by a simple exponential function, the derivative of which at zero time gives the ATP consumption, provided the CCCP treatment affects only and completely the ATP synthesizing reactions during the first seconds but leaves the ATP consuming reactions untouched for a moment. Since the time course of the ATP decay does not differ very much whether 10 or 50 μM CCCP is used, the apparent initial decay of ATP is obviously not controlled by the rate of diffusion of CCCP to its site of action, rather than by the ATP consumption.

Nevertheless, these ATP turnover results do not reflect the entire energy turnover of the cell, because the inhibition of ATP synthesis has not been complete and energy sources different from ATP may be involved as well. So the measured initial ATP decay upon exposure to CCCP will be an underestimate of the total energy available to the cell.

Results

As reported repeatedly [2, 3, 11, 15, 26], the normal resting potential of about −170 mV is much too high for being due to a passive diffusion regime, since the most negative equilibrium potential (of potassium) E_K is only about −90 mV. Since Cl^- influx and the high membrane voltage V_m are affected in a similar way by metabolic stimulation or inhibition and by external Cl^- supply [26], an active electrogenic Cl^- influx has been suggested. Though the significance of the Cl^- fluxes for the electrical properties has to be discussed under some new aspects, this system will be called the (electrogenic) pump P in the following. In order to study the properties of the pump, we have to analyze its role in the entire network of the electrical membrane parameters. Therefore, we tried to isolate specific functions.

Passive Pathways

It was found that such an isolation could be achieved by temperature. When the pump appears to be blocked by low temperatures (below 10 °C), the membrane voltage is at a second stable level of about −80 mV and

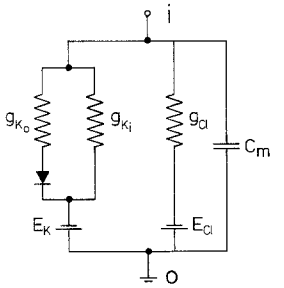

Fig. 1. Equivalent circuit of the passive diffusion system. g_{K_o}, potassium conductance for outward current, about 600 μmho cm^{-2}; g_{K_i}, potassium conductance for inward current, about 13 μmho cm^{-2}; E_K, potassium equilibrium potential, about −90 mV; g_{Cl}, chloride conductance, about 15 μmho cm^{-2}; E_{Cl}, chloride equilibrium potential, about ±0 mV; C_m, membrane capacity, about 5 μF cm^{-2}; *i*, inside (cytoplasm); *o*, outside (seawater)

much more sensitive to external potassium than under normal conditions [11, 26]. This state is in line with a passive diffusion potential with K^+ being the main ion:

$$E_K = -90 \text{ mV} \approx -RT/F \times \ln 400/10. \quad (1)$$

This hypothesis can be tested by resistance measurements. We would expect a 40-fold conductance for outward current compared with inward current [13]. An example is presented in Fig. 4, where the conductance for inward current (hyperpolarizing) is 28 μmho cm^{-2} and the conductance for outward current (depolarizing) is 21 times larger (ca. 600 μmho cm^{-2}). This ratio is smaller than expected (40-fold), partially because the potassium activity inside might be lower than 400 mM, or because there is an additional leak pathway in parallel (Fig. 1). In both cases the passive membrane potential should be lower than −90 mV. The measured value of the diffusion system E_d is about −80 mV or lower.

For the pure potassium system the conductance for inward current would amount to 15 μmho cm^{-2}, that is 2.5% of the high conductance for outward current. The remainder, 13 μmho cm^{-2}, could be attributed to a Cl^- channel. Such a Cl^- pathway ($E_{Cl}=0$, $g_{Cl}=13$ μmho cm^{-2}) in parallel to the K^+ system can, in addition, account for the depolarization from E_K (−90 mV) by about 10 mV to the measured membrane voltage (−80 mV) in the cold. In fact, a Cl^- conductance is likely to exist at low temperatures, because considerable Cl^- fluxes are measured in the cold. Saddler [25] reported 50 pmol cm^{-2} sec^{-1}. If this efflux is independent of other fluxes, a Cl^- conductance

$$g_{Cl} = \Phi_{Cl} F/(E_d - E_{Cl}) \quad (2)$$

of about 60 μmho cm^{-2} would result. Since this value is about 5 times higher than the expected 13 μmho cm^{-2}, and our results yield an even higher conductance (Cl^- efflux about 300 pmol cm^{-2} sec^{-1}), the measured Cl^- efflux cannot represent entirely charge transport between the cytoplasm and outside. One possibility to account for this discrepancy would be electroneutral Cl^- transport together with a counterion; another one will be discussed below.

In order to represent the electrical data of the passive diffusion system, the potassium pathway and a Cl^- pathway with low conductance have to be arranged in parallel (Fig. 1). The diode characteristics of the potassium channel and E_K are due to the concentration difference between inside and outside the cell. Since the concentration gradient for Cl^- is irrelevant [25], the equilibrium potential of Cl^-, E_{Cl}, is about zero and no rectification occurs in the Cl^- pathway.

The membrane capacitance C_m of about 5 μF cm^{-2} has been found to be rather constant under various conditions [15]. The diode element is rather slow (time dependence not represented in the circuit); when switching from one conductance to the other, time constants in the range of 100 msec appear, probably due to redistribution of potassium in the membrane.

Linear Cable

If under normal conditions, small rectangular current pulses are injected into the cell, the observed voltage response V always displays two distinct phases with different time constants [11, 15, 27]. First, there is a small exponential rise in the range of msec, followed by a large one in the range of some seconds. In order to account for this situation, the parameters related to the fast (slow) response will be called "early" ("late") and marked with the superscript "o" ("∞"). Fig. 2 shows two examples of original recordings of the early (A) and the late (B) voltage response at different distances from the electrode injecting square-waved current pulses. The resulting cable properties under L and D conditions, calculated by linear cable theory [19] are compiled in Table 1; these data represent the same experiments as reported before [15]. The resistivity of the cell interior appears to be constant in all four cases, but rather high judged by the ionic content of the cell [25] which would yield a resistivity of about 25 Ωcm. This discrepancy was suggested to be due to the location of the electrode tips in the cytoplasmic compartment, rather than in the vacuole, and due to an appreciable resistance of the tonoplast [15]. The

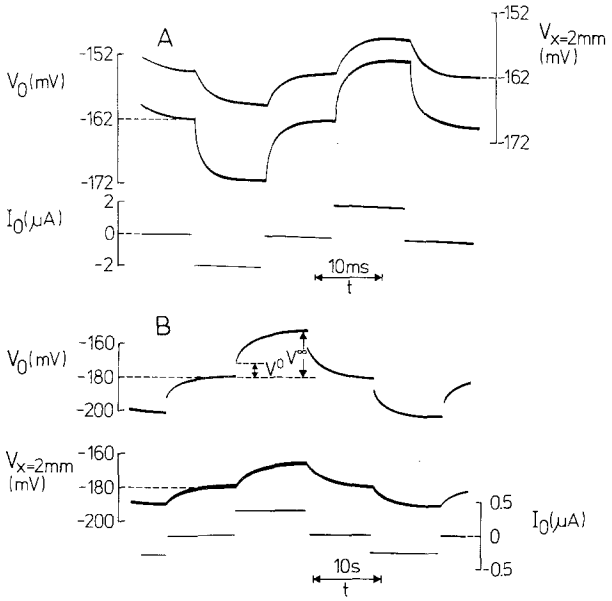

Fig. 2. Voltage course at two different distances ($x=0$ and $x=2$mm) from an electrode, injecting small square-waved current pulses. *A*: early response, V^0; lower trace: injected current; upper two traces: voltage recordings; D, 23 °C. *B*: late response V^∞ after early response V^0; lower trace: injected current; upper traces: voltage recordings; L, 23 °C

late capacitance is too large to be understood as a membrane capacitance; its nature will be discussed below. The late processes do not appear in the cold, when the pump seems to be blocked; therefore, these properties are attributed to the pump *P*.

This typical biphasic voltage response can be simulated by the analog circuit in Fig. 3 *A*. Upon rectangular current pulses, the early voltage

Table 1. Electrical data ± SEM of the *Acetabularia* membrane, obtained by the voltage response upon small rectangular current pulses (comp. Fig. 2)

	Light	Dark
Resting potential V_m (mV)	−180 ±2	−167 ±2
Early conductance g^0 (mmho cm^{-2})	6.25±1.2	3.23±0.4
Late contuctance g^∞ (mmho cm^{-2})	0.63±0.16	0.30±0.08
Early capacity C_m (μF cm^{-2})	5.2 ±0.9	4.8 ±0.6
Late capacity C_P (μF cm^{-2})	3500 ±600	3200 ±500
Early inner resistivity r_i^0 (Ωcm)	39 ±3	38 ±3
Late inner resistivity r_i^∞ (Ωcm)	38 ±8	38 ±9

Results from 7 cells; analysis by linear cable theory [19]. Data rearranged from [15]. 23 °C; Light: 100 mW cm^{-2}; Dark: 0.1 mW cm^{-2} white light.

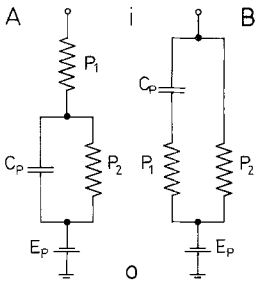

Fig. 3. Two possible circuits to simulate biphasic voltage response upon rectangular current pulses (comp. Fig. 2). Possibility A: $V_{P_1}^{\infty} \neq \text{const}$. Possibility B: $V_{P_1}^{\infty} = 0 = \text{const}$.

drop will occur only across the resistance of the element P_1, as long as the element P_2 is shorted by the capacitance C_P. When this capacitance is charged with the time constant $\tau^{\infty} = R_{P_2} \times C_P$, the voltage will rise up to the voltage drop across the sum of the resistances of P_1 and P_2. As an alternative, the circuit of Fig. 3 B can produce the same biphasic voltage response. However, in this case the late voltage and current across the element P_1 would always be zero. This consequence is in direct contradiction to the finding that the conductance of the element which determines the early response (P_1), is voltage-sensitive (Figs. 4 and 5). Therefore, the model A in Fig. 3 will be used as the pathway responsible for the biphasic voltage course.

Since under normal conditions the entire late membrane conductance is larger than in the cold, we have to arrange this biphasic system as an additional conductance to the passive system, that is in parallel (comp. Figs. 9 and 13). If the passive pathways are not affected by the change from low temperature conditions where the pump is blocked to normal conditions where the pump is operating, the pump currents could be determined simply as the difference between the current of the total system and of the passive system (comp. Fig. 10).

Current-Voltage Relationships

As mentioned above, below 10 °C the current-voltage relationship represents only the passive diffusion system which consists of two linear branches merging near E_K (comp. Figs. 4 and 10). In order to obtain the nonlinear properties of the active pathway, the current-voltage characteristics of the entire system, therefore, have to be studied under normal

temperature where the pump is operating. Since even the input characteristics show a region with negative slope conductance [11, 15], the voltage response upon current clamp cannot give sufficient information, because there exist up to three different voltage values for a current value. Therefore, voltage clamp has to be applied, because the I–V curves display only one current value for each voltage.

The steady-state current-voltage relationships of the membrane $i_m^\infty(V_m)$ presented in Figs. 4 and 5, have been obtained with three microelectrodes close to the cell end [1]. Sufficiently long rectangular voltage-clamp steps V_s have been applied, so the clamp current reached steady state ($t \gg \tau^\infty$). The time course of the clamp current, with initially high values, decreasing with a time constant in the range of seconds (τ^∞), to a lower stable value, confirms the conclusions from the conductance experiments about the organization of the active pathway (Fig. 3). In order to obtain additional information about the element P_1, short ($\tau^0 \ll t \ll \tau^\infty$) voltage pulses V_p of about 10 mV have been superimposed on the voltage-clamp step V_s. The early response of the clamp current i_m^0 upon these voltage pulses V_p gives the early conductance

$$g^0 = i_m^0 / V_p \tag{3}$$

at different clamped voltages V_m. The g^0 values presented in Figs. 4 and 5 are taken at the time when the late clamp current i_m^∞ has reached steady state. A detailed description of this procedure has been presented previously [15].

Fig. 4 shows the results from one cell at 23 °C and 8 °C. The normal dashed lines are extrapolations according to measurements on different cells. The thin dashed line indicates that the extension of the low conductance branch at 8 °C, passes the origin (compare also Fig. 10). Since in the cold the large time constant is missing ($g^\infty = g^0$), the data of $g^0(V_m)$ in the cold are omitted in this Figure. The typical property of the steady-state current-voltage relationship, $i_m^\infty(V_m)$, under normal conditions, is its negative slope for voltages more positive than -140 mV. The large positive conductance below E_K (indicated in Fig. 4 by a dashed line) turns out to be about the same under normal conditions and in the cold [11, 15]. For hyperpolarization, the current-voltage relationship is rather linear, but for larger deviations, a slight decrease of the slope can be observed. These I–V curves for normal and low temperatures intersect at about -190 mV.

The early conductance g^0 decreases for depolarization and amounts to only about 5% of the control value at -100 mV. For hyperpolarization,

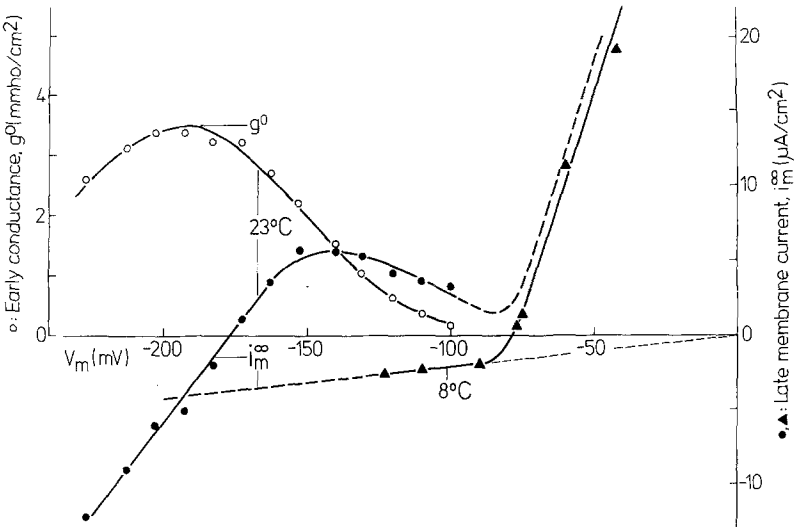

Fig. 4. Example of steady-state current-voltage relationships (right ordinate) of the membrane; ●—●, D at 23 °C; ▲—▲, D at 8 °C. Left ordinate: early conductance g^0, (o—o), as function of the steady-state membrane voltage V_m. Voltage clamp experiments on one cell. Square-waved voltage clamp steps (ca. 30 sec) with superimposed pulses (ca. 10 mV, 0.5 sec). Normal dashed lines are extrapolations according to results of other cells; thin dashed line indicates that the extension of the low conductance branch at 8 °C passes the origin

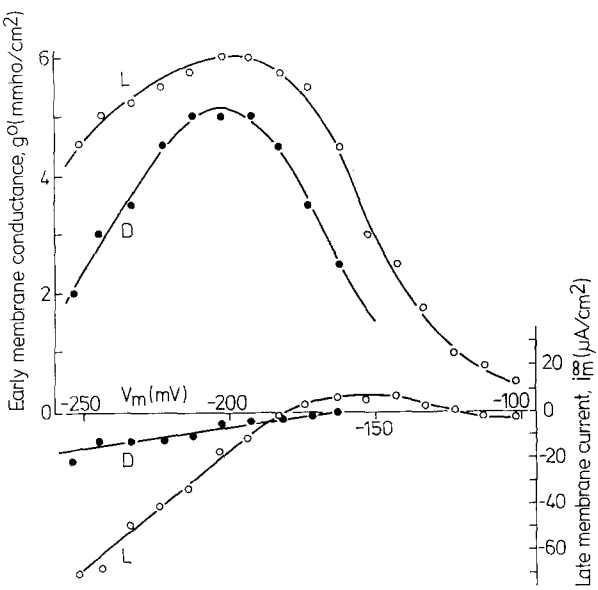

Fig. 5. Example of steady-state current-voltage relationships of the membrane (right ordinate, lower two curves); ●—●, D; o—o, L. Left ordinate, upper two curves: early conductance g^0 as function of the steady-state membrane voltage V_m. Voltage clamp experiment on one cell. 23 °C

g^0 rises to a maximum at about -200 mV, close to the intersection of the steady state I–V curves under normal and low temperature conditions (-190 mV). For larger hyperpolarizations g^0 decreases again.

In Fig. 5 the steady-state current-voltage relationship and the voltage dependence of g^0 of one cell is given under D and L conditions. In this example, the investigated voltage range is more negative than E_K. So the steep conductance increase below E_K is missing in Fig. 5. The current-voltage relationship, $i_m^\infty(V_m)$, confirms qualitatively the results from the conductance measurements (Table 1). Light raises the resting potential and the conductance g^∞. The two I–V curves from L and D conditions intersect again at about -190 mV. The early conductance g^0 turns out to be not only voltage sensitive as in Fig. 4, but also sensitive to light. Under illumination, the peak conductance has not shifted its location at about -200 mV, but is about 20% higher than the D control. The finding that the early conductance at the resting potential (here, D: -163 mV, L: -181 mV) is about doubled by light (here, D: 2.5 mmho cm^{-2}, L: 5.8 mmho cm^{-2}) agrees well with the data of V_m and g^0 in Table 1.

Ion Fluxes

In order to analyze the electrical membrane parameters in terms of the properties of the particular ion pathways, flux measurements have been carried out. No ion other than K^+ and Cl^- has been found to affect the resting potential [11]. Even H^+ appears to be ineffective, because V_m is insensitive to external pH between pH 4 and 9. It should be recalled, however, that the vacuolar pH is only 2.5; so the equilibrium potential of H^+, E_H, between the vacuole and outside is about -300 mV [15]. In addition, *Acetabularia* cells seem to regulate their external pH at about 7.9, the pH of seawater [5]; therefore, there must be a considerable movement of protons (or equivalents) across the membrane. However, for the above reasons, in the present study the role of H^+ will be neglected.

Efflux measurements of K^+ ($^{86}Rb^+$) have shown that under normal conditions the K^+ efflux is very voltage-dependent [24]. According to the diode characteristics of the potassium diffusion system [13], there is a large K^+ efflux at voltages less negative than $E_K = -90$ mV, where a net K^+ efflux should occur along the electrochemical gradient; and for voltages more negative than E_K, a net K^+ influx is expected. Hence, in this voltage range, K^+ ions leaving the cell, cannot be transported by the electrochemical gradient, rather than by different mechanisms, probably K^+/K^+ exchange diffusion. Such a K^+ efflux is measured (2 pmol cm^{-2}

sec^{-1} at -170 mV). Due to the superimposed electrochemical K^+ influx, the apparent K^+ efflux increases slightly for depolarization down to E_K and increases drastically at voltages more positive. In fact this voltage-dependent change of K^+ efflux turned out to be stimulated by about the factor 40 at voltages more positive than E_K [24].

The net influx down the electrochemical gradient via the potassium pathway with a conductance of 15 μmho cm^{-2} (computation see above) should be

$$\Phi_{K_i} = (E_m - E_K) g_{K_i} / F \tag{4}$$

that is about 14 pmol cm^{-2} sec^{-1} at the resting potential. This value compares well with the measured K^+ influx of 10–40 pmol cm^{-2} sec^{-1} [24, 25], which implies some pmol cm^{-2} sec^{-1} K^+ influx due to K^+ exchange. In conclusion, the potassium conductance under normal conditions is rather low compared with the entire membrane conductance (Table 1), and there is no reason to assume drastic temperature-sensitive changes of the K^+ pathway, since there is good agreement between the fluxes calculated from the conductance measurements in the cold and the flux measurements at normal temperatures.

As for the Cl^- fluxes, there has been general agreement among different authors [11, 26] that the Cl^- ion plays a dominant role in the *Acetabularia* membrane, because the measured in- and effluxes are very high (200–2,000 pmol cm^{-2} sec^{-1}) and appear to be correlated with the membrane potential [16, 26]. However, there are complications in the details. The rather "low" fluxes reported by Saddler [25] do not follow the biphasic efflux kinetics (except for 5 °C) found by Gradmann *et al.* [16] and Gläsel and Zetsche [10] who obtained larger (not significant on statistical grounds) Cl^- fluxes according to the model of three compartments in series. It seems to be possible that in Saddler's experiments the tonoplast was not intact, and the two compartments of the cytoplasm and the vacuole appear to be fused to one compartment. Furthermore, the Cl^- efflux is much more sensitive to voltage-affecting external conditions like temperature [26] and light [16, 26] to obey just the electrochemical gradient for Cl^-. One example is given by Fig. 6, where during the fast phase (after the washout of the cell wall during the first minutes), the efflux is stimulated by the factor 1.6 (mean 1.8 ± 0.5) in the light which raises the membrane voltage ($E_m - E_{Cl}$) only by about 6% (Table 1).

Suppose the Cl^- fluxes are carrying charge across the plasmalemma, the results (comp. Table 2) imply that the Cl^- conductance cannot be assumed to be constant in different states of activity of the electrogenic

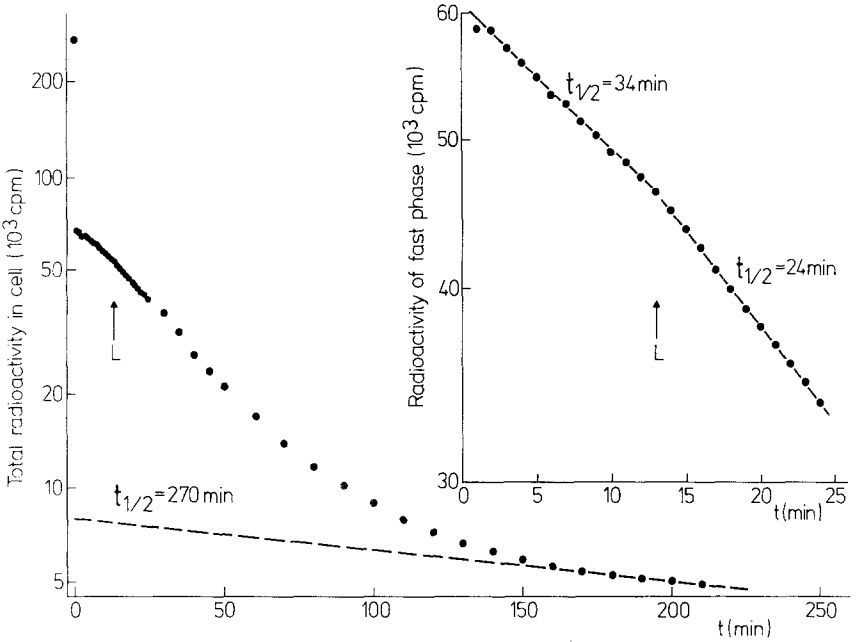

Fig. 6. Example of Cl^- washout kinetics. Dashed line indicates extrapolation of slow phase to zero time. Note amount of radioactivity in the fast (6.2×10^4 cpm) and in the slow (0.8×10^4 cpm) phase at the beginning. Inset: radioactivity of fast phase alone as difference between the entire radioactivity and the radioactivity of the slow phase (extrapolation). Arrows mark beginning of L conditions. 23 °C

Table 2. Chloride efflux ±SEM of the fast phase Φ_v, probably from the vacuole and of the slow phase Φ_c, probably from the cytoplasm under D and L conditions

	Light	Dark
Φ_v (pmol cm^{-2} sec^{-1})	1260±800	770±400
Φ_c (pmol cm^{-2} sec^{-1})	130±80	70±40

pump (D and L conditions). If one calculates this passive conductance by Eq. (2), it turns out to be even higher (D: 400, L: 700 μmho cm^{-2}) than the entire membrane conductance, including the active pathways (Table 1). One possibility to account for this paradox is to assume as above that only a fraction of the Cl^- efflux is a net ion flux, the remainder being due to electroneutral transport. The calculation of the numerical values of the elements in the analog circuit (Fig. 9) under these conditions will be presented in the discussion (Table 4A).

There is, however, another possibility to explain the enormous size of Cl^- fluxes. In the analysis of the biphasic washout kinetics (Fig. 6) the

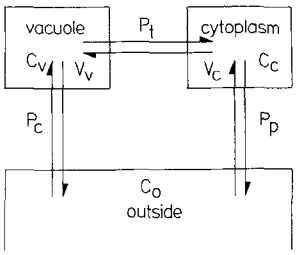

Fig. 7. Model of compartments and pathways for the Cl^- fluxes in *Acetabularia*. $C_{v,c,o}$, concentrations in vacuole, cytoplasm and outer medium. $V_{v,c}$, volume of vacuole and cytoplasm, volume of outer medium taken for ∞. $P_{t,p,c}$, permeabilities of tonoplast, plasmalemma and cytoplasm (the latter representing a direct pathway from vacuole to outer medium, bypassing tonoplast and plasmalemma)

fast phase is attributed to the efflux from the cytoplasm to the outer medium and the slow phase to the efflux out of the vacuolar compartment. Linear extrapolation of the semilogarithmic plots to $t=0$ yields the amount of labeled Cl^- in the vacuolar (slow phase) and cytoplasmic (fast phase) compartment. For cells equilibrated with the outer medium (1 cpm = 1.25×10^{-11} mol Cl^-) the amount of Cl^- in the particular compartments can be obtained immediately. If we apply this calculation to our data, the amount of Cl^- in the "cytoplasmic" phase exceeds usually the amount in the "vacuolar" phase. Since the cytoplasm occupies only about 10% of the entire cell volume [25], enormous Cl^- concentrations (more than 3 M) would have to be assumed for the cytoplasm and very low ones for the vacuole, in contrast to the directly measured concentrations which are approximately the same in both compartments [25]. An extreme example is given by Fig. 6, where at $t=0$ the radioactivity is about 8 times as high in the fast compartment as in the slow one. Therefore, the question arises whether the standard flux analysis is appropriate for *Acetabularia*.

As an alternative, it is suggested that there is an additional direct Cl^- pathway from the vacuole to the outer medium, bypassing tonoplast and plasmalemma (Fig. 7). The time course of the tracer efflux out of the vacuolar compartment, $\Phi_v^*(t)$ and out of the cytoplasm, $\Phi_c^*(t)$, would be

$$\Phi_v^*(t) = \frac{C_0^*(P_c P_t + P_c P_p + P_t P_p)}{(P_t + P_p)} \exp\left(\frac{-t(P_c P_t + P_c P_p + P_t P_p)}{(P_t + P_p) V_v}\right) \tag{5}$$

$$\Phi_c^*(t) = \frac{C_0^*(P_c P_t + P_c P_p + P_t P_p)}{(P_c + P_t)} \exp\left(\frac{-t(P_c P_t + P_c P_p + P_t P_p)}{(P_c + P_t) V_c}\right) \tag{6}$$

where C_0^* is the initial tracer concentration (about the same in the vacuole and in the cytoplasm), $P_{c,t,p}$ are the permeabilities of the cytoplasm (for

the direct flux from the vacuole to the outer medium), the tonoplast and the plasmalemma, respectively, V_v and V_c are the volumes of the vacuole and cytoplasm.

These two equations (5) and (6) can be drawn from the two straight lines of the semilogarithmic plot of the washout kinetics (compare Fig. 4). However, they are not sufficient to determine the three unknown permeabilities P_c, P_t and P_p. Even additional conductance measurements do not give the missing information, since g^∞ depends linearly on P. Furthermore, the Cl^- transport system from the vacuole to the outside is unlikely to be a simple diffusion process, and its treatment as a permeability (P_t) might be inappropriate.

Another question is whether this direct Cl^- transport from the vacuole to the outside is peculiar to Cl^- or reflects an unspecific leak. In the latter case, the release of any tracer from the vacuole should have similar kinetics to the fast phase of the Cl^- washout ($t_{1/2}$ about 20 min). The efflux kinetics of K^+ ($^{86}Rb^+$), however, do not exhibit this characteristic [24]. Therefore, it is concluded that the high Cl^- fluxes from (and to) the vacuole are not artifacts by injury due to the measuring treatment, but mediated by specific Cl^- pathways, maybe by vesicles, as has been suggested for *Characean* cells by MacRobbie [21]. This interpretation is consistent with the fact that in the *Acetabularia* vacuole various compounds are accumulated (H^+, K^+, oxalate ...); only the Cl^- concentration is about the same inside and outside.

It is still possible that the measured fluxes are not entirely charge-carrying; as mentioned above, electroneutral Cl^- exchange may take place which has been postulated to occur in *Chaetomorpha* [8]. The Cl^- currents may also be (partially) neutralized by cations like H^+, because light-sensitive H^+ transport in *Acetabularia* is reported as well [5]. At present, the data about the Cl^- fluxes in *Acetabularia* are not clear enough as to provide quantitative evidence for the electrical properties of the plasmalemma membrane.

ATP, Content and Turnover

Another attempt to obtain more information about the electrogenic pump is to study its relationship to the energy metabolism of the cell. Therefore some ATP experiments have been carried out. Within one set of experiments, the steady-state ATP level appears to be rather con-

Table 3. Content and consumption of ATP ± SEM under different conditions

	Light	Dark	Cold
Content (pmol per mg d.w.)	431 ± 22	459 ± 33	483 ± 18
Density ($\mu Ws\ cm^{-2}$)	41 ± 2	43 ± 3	46 ± 2
Energy in C_P ($\mu Ws\ cm^{-2}$)	55 ± 8	46 ± 5	–
Consumption (pmol sec^{-1} per mg d.w.)	311 ± 37	201 ± 32	61 ± 20
($\mu W\ cm^{-2}$)	29 ± 4	19 ± 3	6 ± 2

Light: 100 mW cm^{-2}; Dark: 0.1 mW cm^{-2} white light; 23 °C; Cold: 0 °C. Average cell length 2.5 cm, diameter 0.25 mm. For conversion, 1 mol ATP taken for 4.2×10^4 Ws.

stant under various conditions (Table 3). If we take an ATP content of 460 pmol mg^{-1} dry weight for normal, the concentration in the entire cell, related to the cell volume, will be about 0.17 mM or 1.7 mM in the cytoplasm at a volume ratio of 10:1 between cell volume and cytoplasm. Since the cytoplasm is mainly located at the periphery of the cell, it is appropriate to relate the ATP content to the cell surface. These units are useful for a comparison of the ATP metabolism with membrane parameters. For discussion of the energetics, the free energy of the hydrolysis of 1 mol ATP will be taken for 10 kcal $\triangleq 4.2 \times 10^4$ Ws, as a crude estimate, and the ATP data are listed not only in pmol per mg dry weight but also converted to energy units per membrane area ($Ws\ cm^{-2}$) in Table 3.

From the results of the ATP content under different conditions (Table 3) it is evident that the cell successfully maintains a constant ATP level. This feedback system may even overcompensate, since under low energy conditions (5 °C) the ATP content can be even higher and under bright light even lower than in the control. The steady-state ATP level is, therefore, no useful indicator for the actual state of energy of the cell.

More information is expected from the ATP turnover which in fact turned out to be rather sensitive to external conditions. Fig. 8 shows an example of the ATP decay upon sudden inhibition of phosphorylation by CCCP. The inhibition is not complete (60%), despite the high CCCP concentration. Some ATP is apparently provided from CCCP insensitive phosphorylation (fermentation, glycolysis ...). The postulated ATP-regulating system may be involved, since the time course of the ATP decay in CCCP is strictly not a simple exponential function; a damped oscillation can be superimposed as indicated by the dashed line in Fig. 8. Such a feedback system has already been discussed for *Neurospora* [31].

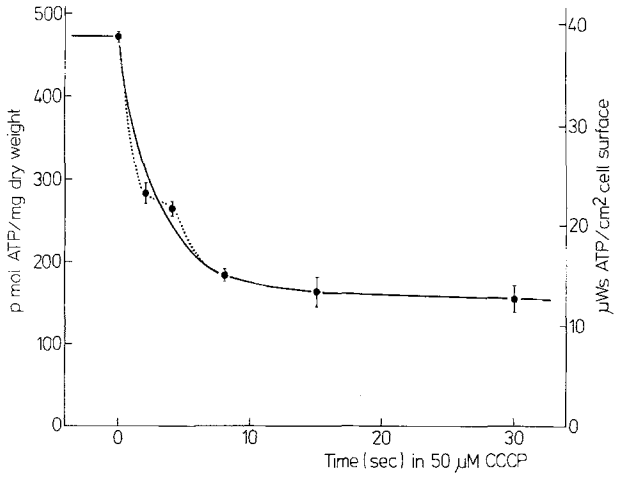

Fig. 8. Example of an experiment to determine ATP turnover. Left ordinate: ATP content in pmol per mg dry weight; right ordinate: ATP content in μW sec cm^{-2}, 1 mol ATP $\hat{=}$ 4.2 $\times 10^4$ Ws; abscissa: time in 50 μM CCCP. Vertical bars mark $\pm$SEM. Solid line: smooth curve, the derivative of which at zero time is taken as a measure for the ATP turnover; dotted line through the measured points indicates damped oscillations superimposed on the exponential ATP decay

If we fit the measured ATP decay by a simple exponential function, its derivative at zero time can be used as a measure for the normal ATP consumption. The mean values $\pm$SEM of the ATP turnover, determined by this procedure, are given in Table 3. Bright light enhances the ATP turnover by 50%, and in the cold, when we expect the metabolism to slow down, the ATP consumption is drastically reduced.

It has to be noted that there are appreciable (up to factor 3) diurnal variations of the ATP turnover, which are in line with the diurnal time course of O_2 evolution [22]. Therefore, only data from the same diurnal phase could be compared. Though no circadian rhythm could be observed in the time course of the resting potential (and the ATP concentration), it may well exist in some current-voltage relationship. However, due to the wide variation of these data, diurnal changes have not been pursued systematically.

Discussion

The stimulated *Acetabularia* membrane exhibits several interesting, time-dependent phenomena, like a fast voltage response upon light [29], action potentials [11, 16] or temporary variation of the Cl^- fluxes [16]. These reactions are probably closely related to the properties of the

particular elements of the analog circuit. However, it is beyond the limits of this study to discuss the relationship of these phenomena to the electrical analog circuit in detail. This discussion is confined to the steady-state properties. Before we expound the entire circuit, the properties of some individual elements should be discussed, including their physical meaning.

The Large Capacity C_P

There is a common way to account for the large time constants in the electrical experiments. Unstirred layers in the cell wall with slow depletion of mobile charges could produce slow voltage responses [2, 3]. Such layers in the *Acetabularia* cell wall, however, are unlikely to exist, because the high ionic strength of the seawater outside will provide a high conductance of the cell wall, in contrast to the corresponding situation of *Characean* cells in pond water. Direct evidence against an unstirred-layer effect is the finding that the large time constants are closely related to the operation of the electrogenic pump. In the cold, for instance, when the pump is normally blocked, the slow response cannot be observed. In terms of the analog circuit, g_{P_1} is so small in the cold that C_P is practically disconnected from the point where the voltage is recorded.

Since the model for passive Cl^- fluxes (Fig. 7), with its two storage elements and three conducting elements, is formally similar with the crude electrical model of Fig. 9 (two storage elements C_m and C_P and three conducting elements g_d, g_{P_1} and g_{P_2}), it has to be stated explicitly that two completely different systems are concerned. For instance, the storage elements in the tracer flux model, the volumes of the cytoplasm and of the vacuole, are reflected in the analog circuit as ideal conductances; and the time constants in the tracer flux model are even much larger than in the electrical model. Therefore, it cannot be concluded that the apparent

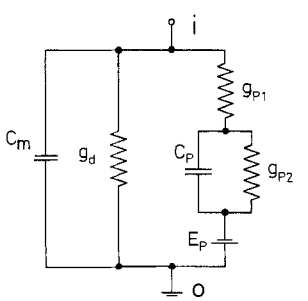

Fig. 9. Simplified analog circuit for voltages more negative than −100 mV. Passive diffusion pathways are summarized in g_d

large capacity C_P of the electrical circuit is simply due to the particular compartmentation of the *Acetabularia* cell.

As a third possibility to account for the large time constants in the electrical behavior, it is suggested that the apparent large capacitance of C_P represents a storage element of metabolic energy, probably the ATP pool. If this hypothesis holds, the amount of energy stored as ATP in the cell should be reflected by the equivalent electrical energy stored in the capacity of C_P in the analog circuit. The experimental data of the ATP concentrations, converted to units of energy per membrane area and the data from the analog circuit,

$$\text{energy} = 0.5\, C_P \times V_{P_2}^2 \tag{7}$$

are compiled for comparison in Table 3. The fair agreement between these two energy values favors the hypothesis that the ATP pool of the cell stands for the capacitance C_P in the electrical behavior. Furthermore, the close relationship between ATP and C_P is supported by the finding that these two parameters, in contrast to other elements, are rather independent of light. The insignificant discrepancy between the two energy data can be due to the underestimate of the free energy of the ATP hydrolysis.

Numerical Data of the Analog Circuit

From the voltage and conductance values of Table 1 some values can be obtained. For voltages more negative than E_K, the diffusion channel, including potassium and chloride conductance, can be regarded as a linear pathway passing the origin (compare Figs. 4 and 10). With this simplification the diffusion pathway can be described by a conductance g_d, without an electromotive force (Fig. 9). In steady state, the pump channel, in parallel to g_d, consists of the electromotive force E_P with its inner conductance g_P. By the measurement of only the membrane voltage V_m and the late conductance g^∞ we are not able to determine the three parameters g_d, g_P and E_P. Based on the limiting assumptions, the following cases *A* and *B* give reasonable results, and will be pursued.

A. We accept from the Cl^- flux data (Table 2) that the diffusion channels change their conductance under bright illumination. E_P can be taken as constant, since the electrogenic pump is probably a mechanism of chemical reactions, the free energy of which is converted to an electrical potential difference across the membrane. The results of this case *A* are given in part *A* of Table 4. The most important consequence of this case

Table 4. Calculation of the steady-state conductance of the diffusion pathway g_d, of the pump conductance g_P, of the electromotive force of the pump E_P, of the power of the pump P_P, and the ratio between the power of the pump and the ATP turnover (compare Table 3), based on the data in Tables 1 and 2 and the assumptions *A*: $g_d = k\Phi_{Cl}$, E_P = const; and *B*: g_d = const, E_P = const.

	A		*B*	
	L	D	L	D
g_d (μmho cm^{-2})	238	109	28	28
g_P (μmho cm^{-2})	388	196	598	277
E_P (mV)	−473	−473	−188	−188
P_P (μW cm^{-2})	20.3	8.8	0.95	0.89
(% ATP consum)	70	46	3.3	4.7

is the high value of $E_P = -473$ mV, which would favor a 1:1 stoichiometry between electrogenically transported charge and ATP, since the standard free energy of the hydrolysis of one molecule of ATP is about 0.44 eV, for a caloric equivalent of 10 kcal mol^{-1}. Changes of the ATP concentration are small (Table 3) and would only contribute 58 mV for a 10-fold change. The power of the pump

$$\text{power}_P = i_P \times E_P \tag{8}$$

would amount to about half of the total energy turnover as ATP is concerned (Table 3). For the fraction of the total energy supply used for transport, values of 0.3% have been reported for *Griffithsia* [20] and ca. 30% for *Neurospora* [30]. Besides this high energy requirement, case *A* yields another difficulty concerning the current-voltage relationship of the element P_1. If E_P is −473 mV, the voltage across this element does not change its sign within the measured range of V_m (up to −300 mV); so the conductance at zero current remains unknown and displays a strange voltage dependence.

B. We disregard the complicated situation about the Cl^- pathways and assume the passive diffusion conductance $g_d = 28$ μmho cm^{-2} as constant (i.e. insensitive to light and temperature). The results in this case are listed in part *B* of Table 4. The conductance change is now only due to the changes in the pump pathway. In this case, the electromotive force of the electrogenic pump E_P amounts to about −200 mV. This value suggests a stoichiometry of 2:1 between translocation of charges and ATP. This stoichiometry has already been suggested for the electrogenic H^+ pump in *Neurospora* [30] and *Characean* cells [33]. The values from Eq. (8) for the power of the pump are much smaller in case *A* because a) E_P is lower and b) the pump current does not drive large Cl^- fluxes.

Furthermore, the element P_1 has its maximum conductance at about -200 mV (Figs. 4 and 5), that is at zero current of case *B*. The theoretical model for a carrier-mediated electrogenic pump [9] predicts maximum conductance at zero current and saturation for large voltage displacements, which is in good agreement with our findings. Therefore, we want to refer to this case *B*.

Nonlinear Elements

Fig. 10 shows a continuous I–V recording, obtained by a voltage-clamp experiment with ramp-shaped time course of the test voltage. Subtraction of the current $i_d(V_m)$ of the diffusion channel (dashed line from another typical experiment under low temperature) from the measured total current, $i_m^\infty(V_m)$, drawn by a solid line, yields the steady-state pump current $i_P^\infty(V_m)$, which is zero at about -190 mV, the electromotive force of the pump, as already reported [15]; $i_P^\infty(V_m)$ is marked as a dotted line in Fig. 10.

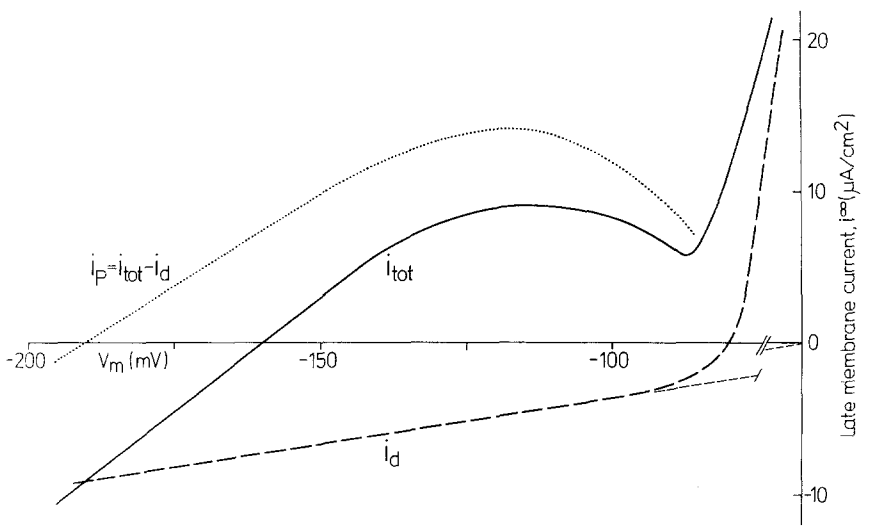

Fig. 10. Determination of the steady-state current-voltage relationship of the pump pathway $i_P(V_m)$ (dotted curve), as the current difference between the entire current-voltage relationship $i_{tot}(V_m)$ of the complete system (solid line) at normal temperature and the current-voltage relationship of the passive diffusion system $i_d(V_m)$ alone at low temperatures (dashed line). Voltage-clamp experiment; continuous current recording upon ramp-shaped test voltage. Hysteresis eliminated by averaging. Solid and dashed curve from different cells. Thin dashed line indicates that the extension of the low conductance branch at low temperatures passes the origin

From the superimposed early conductance measurement g^0 (comp. Figs. 4 and 5)

$$g_{P_1}(V_m) = g^0(V_m) - g_d(V_m), \tag{9}$$

a current-voltage relationship $i_{P_1}(V_m)$ has been calculated by integration of g_{P_1} in V_m [15]. This function, $i_{P_1}(V_m)$, does not give the desired current-voltage relationship of the element P_1, because one must integrate g_{P_1} in V_{P_1}, the voltage only across the element P_1 itself, rather than the voltage V_m across the entire membrane. This voltage $V_{P_1}(V_m)$ can be obtained by the voltage division in the pump channel

$$V_{P_1}(V_m) = (E_P - V_m)\, g_P^{\infty}(V_m)/g_{P_1}(V_m), \tag{10}$$

where $g_P^{\infty}(V_m)$ is the chord conductance of the entire active pathway (the derivative of the dotted line in Fig. 10). The current-voltage relationship of the pump P_1 itself can now be calculated as

$$i_{P_1}(V_{P_1}) = \int g_{P_1}(d\,V_{P_1}) + c, \tag{11}$$

where c is a constant current, providing that $i_{P_1}(V_{P_1})$ passes the origin at -190 mV. An example of the resulting current-voltage relationship of this element is given by Fig. 11 for D and L conditions, based on the data from Fig. 5. Saturation could not be reached in this experiment, but

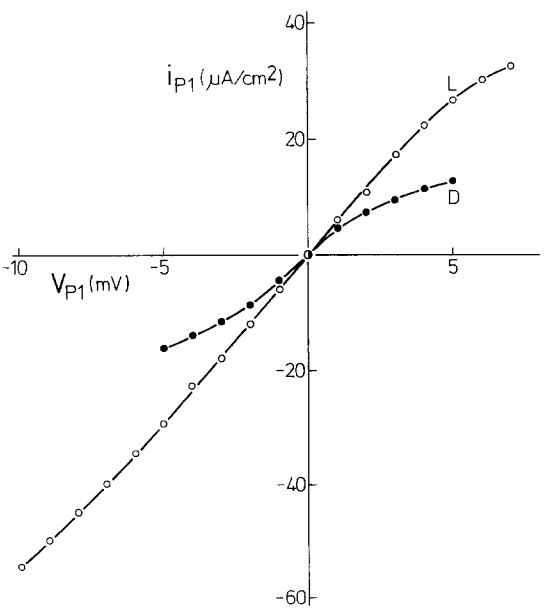

Fig. 11. Example of the steady-state current-voltage relationship $i_{P_1}(V_{P_1})$ of element P_1; obtained by integration of $g^0_{P_1}$ in V_{P_1}. Data from experiment of Fig. 6. o—o, L; ●—●, D. 23 °C

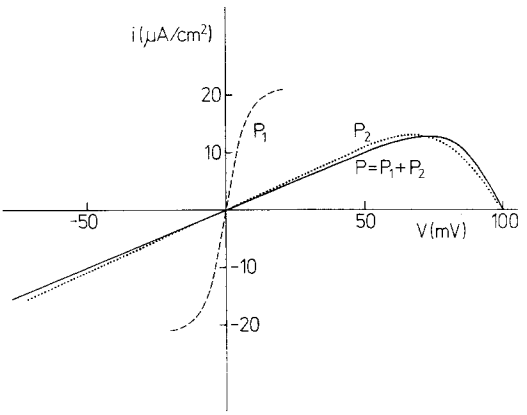

Fig. 12. Determination of the steady-state current-voltage relationship of the element P_2, $i_{P_2}(V_{P_2})$ (dotted line), as the voltage difference between the current-voltage relationship of the entire pump pathway $i_P(V_m)$ (solid line) and the current-voltage relationship of the pump element P_1, $i_{P_1}(V_{P_1})$ (dashed line). Solid line according to data in Fig. 10; dashed line extrapolated according to data in Fig. 11. 23 °C, D

extrapolation would yield a saturation current of about 25 μA cm^{-2} in D and 60 μA cm^{-2} in L.

Since the known current-voltage relationship $i_P^\infty(V_m)$, respectively, its inverse (voltage-current) function $V_m(i_P^\infty)$, of two elements in series, is the voltage sum of its components $V_{P_1}(i_P^\infty)$ and $V_{P_2}(i_P^\infty)$, we are able to calculate the voltage-current relationship of the element P_2 alone as

$$V_{P_2}(i_P^\infty) = V_P(i_P^\infty) - V_{P_1}(i_P^\infty), \tag{12}$$

respectively, its inverse function $i_{P_2}^\infty(V_{P_2})$, since $i_P^\infty = i_{P_1}^\infty = i_{P_2}^\infty$. This derivation is illustrated by Fig. 12. Here the voltage difference between the entire pump system (solid line) and P_1 (dashed line) gives the voltage of P_2 for each current value (dotted line). The resulting current-voltage relationship does not differ much from the characteristics of the entire pump system, because the voltage drop across P_1 is small compared with the voltage across P_2.

The physical meaning of the element P_2 and its current-voltage relationship with the negative slope conductance for voltages more positive than −140 mV, is not clear yet. However, in terms of the analog circuit, the increase of V_m by photosynthetically active light [28] is due to a conductance increase of P_2. Therefore, P_2 is suggested to reflect phosphorylating reactions. As already discussed, P_1 is suggested to be the electrogenic pump itself.

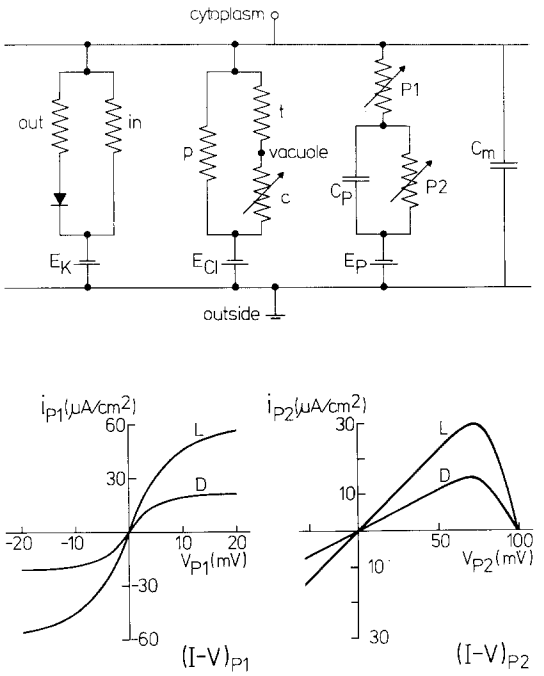

Fig. 13. Upper part: detailed analog circuit of the *Acetabularia* membrane. Data of constant and linear elements in Table 5; arrows mark variable elements. Lower part: current-voltage relationships (semischematically) of the nonlinear and light-sensitive elements P_1 and P_2

Table 5. Set of possible numerical values of the particular linear and constant elements of the analog circuit (Fig. 13)

g_{K_i} (μmho cm^{-2})	15	E_K (mV)	−90
g_{K_0} (μmho cm^{-2})	600	E_{Cl} (mV)	±0
$g_{Cl,p}$ (μmho cm^{-2})	12	E_P (mV)	−190
$g_{Cl,t}$ (μmho cm^{-2})	1	C_m (μF cm^{-2})	5
$g_{Cl,c}$ (μmho cm^{-2})	500	C_P (μF cm^{-2})	3000

$g_{Cl,t}$ and $g_{Cl,c}$ are estimates; $g_{Cl,c}$ may be sensitive to light and temperature.

For a survey, the complete and detailed analog circuit is given by Fig. 13 together with the current-voltage relationships of its nonlinear elements P_1 and P_2 under D and L conditions. As far as available, the numerical values of the linear elements are compiled in Table 5. Though it has not been possible yet to determine each numerical value from one individual cell nor from several cells with statistical significance, this circuit is suggested to be a consistent representation of the electrical properties of the *Acetabularia* membrane in steady state.

This work was supported by a research grant from the Deutsche Forschungsgemeinschaft.

References

1. Adrian, R.H., Chandler, W.K., Hodgkin, A.L. 1970. Voltage clamp experiments in striated muscle fibres. *J. Physiol.* **208**:607
2. Barry, P.H., Hope, A.B. 1969*a*. Electroosmosis in membranes: Effects of unstirred layers and transport numbers. I. Theory. *Biophys. J.* **9**:700
3. Barry, P.H., Hope, A.B. 1969*b*. Electroosmosis in membranes: Effects of unstirred layers and transport numbers. II. Experimental. *Biophys. J.* **9**:729
4. Beth, K. 1953. Experimentelle Untersuchungen über die Wirkung des Lichtes auf die Formbildung von kernhaltigen und kernlosen *Acetabularia*-Zellen. *Z. Naturforsch.* **8b**:334
5. Brändle, E.P.O., Kötter, R., Zetsche, K. 1975. Changes of pH in culture solution of *Acetabularia* caused by proton flux. *Protoplasma* **83**:173
6. Cole, K.S. 1961. Non-linear current-potential relations in an axon membrane. *J. Gen. Physiol.* **44**:1055
7. Cram, W.J. 1968. Compartmentation and exchange of chloride in carrot root tissue. *Biochim. Biophys. Acta* **163**:339
8. Findlay, G.P., Hope, A.B., Pitman, M.G., Smith, F.A., Walker, N.A. 1971. Ionic relations of marine algae. III. *Chaetomorpha:* Membrane electrical properties and chloride fluxes. *Aust. J. Biol. Sci.* **24**:731
9. Finkelstein, A. 1964. Carrier model for active transport of ions across a mosaic membrane. *Biophys. J.* **4**:421
10. Gläsel, R.M., Zetsche, K. 1975. ^{36}Chloride fluxes of *Acetabularia. Protoplasma* **83**:175
11. Gradmann, D. 1970. Einfluss von Licht, Temperatur und Aussenmedium auf das elektrische Verhalten von *Acetabularia. Planta* **93**:323
12. Gradmann, D. 1974. Wirkung des Lichts auf die elektrogene Pumpe von *Acetabularia.* Zusammenfassungen der Vorträge zur Tagung der Deutschen Botanischen Gesellschaft, Würzburg: **70**
13. Gradmann, D., Bentrup, F.W. 1970. Light-induced membrane potential changes and rectification in *Acetabularia. Naturwissenschaften* **57**:46
14. Gradmann, D., Bokeloh, G. 1975. Energy consumption of the electrogenic pump in *Acetabularia mediterranea. Protoplasma* **83**:172
15. Gradmann, D., Klemke, W. 1974. Current-voltage relationship of the electrogenic pump in *Acetabularia. In:* Membrane Transport in Plants. U. Zimmermann and J. Dainty, editors. p. 131. Springer-Verlag, Berlin-Heidelberg-New York
16. Gradmann, D., Wagner, G., Gläsel, R.M. 1973. Chloride efflux during light-triggered action potentials in *Acetabularia mediterranea. Biochim. Biophys. Acta* **323**:151
17. Hämmerling, J. 1944. Zur Lebensweise, Fortpflanzung und Entwicklung verschiedener Dasycladaceen. *Arch. Protistenk.* **97**:7
18. Hogg, J., Williams, E.J., Johnston, R.J. 1968. A simplified method for measuring membrane resistances in *Nitella translucens. Biochim. Biophys. Acta* **150**:518
19. Hogg, J., Williams, E.J., Johnston, R.J. 1969. The membrane electrical parameters of *Nitella translucens. J. Theoret. Biol.* **24**:317
20. Lilley, R.McC., Hope, A.B. 1971. Chloride transport and photosynthesis in cells of *Griffithsia. Biochim. Biophys. Acta* **226**:161
21. MacRobbie, E.A.C. 1969. Ion fluxes to the vacuole of *Nitella translucens. J. Exp. Bot.* **20**:236
22. Mergenhagen, D., Schweiger, H.G. 1974. Circadian rhythmicity: Does intercellular synchronization occur in *Acetabularia*? *Plant Sci. Lett.* **3**:387
23. Mitchell, P. 1961. Coupling of phosphorylation to electron and hydrogen transfer by a chemiosmotic type of mechanism. *Nature* **191**:144

24. Mummert, H., Gradmann, D. 1976. Correlation of potassium fluxes and electrical properties of the membrane of *Acetabularia. (In preparation)*
25. Saddler, H.D.W. 1970*a*. The ionic relations of *Acetabularia mediterranea. J. Exp. Bot.* **21**:345
26. Saddler, H.D.W. 1970*b*. The membrane potential of *Acetabularia mediterranea. J. Gen. Physiol.* **55**:802
27. Saddler, H.D.W. 1971. Spontaneous and induced changes in the membrane potential and resistance of *Acetabularia mediterranea. J. Membrane Biol.* **5**:250
28. Schilde, C. 1966. Zur Wirkung des Lichtes auf das Ruhepotential der grünen Pflanzenzelle. *Planta* **71**:184
29. Schilde, C. 1968. Schnelle photoelektrische Effekte der Alge *Acetabularia. Z. Naturforsch.* **23b**:1369
30. Slayman, C.L., Long, W.S., Lu, C.Y.-H. 1973. The relationship between ATP and an electrogenic pump in the plasma membrane of *Neurospora crassa. J. Membrane Biol.* **14**:305
31. Slayman, C.W., Rees, D.C., Orchard, P.P., Slayman, C.L. 1975. Generation of adenosine triphosphate in cytochrome-deficient mutants of *Neurospora. J. Biol. Chem.* **250**:396
32. Strehler, B.L. 1970. Adenosin-5-triphosphat und Creatinphosphat Bestimmung mit Luciferase. *In:* Bergmeyer, Methoden der Enzymatischen Analyse. U.H.Bergmeyer, editor. Vol. 2, p. 2036. Verlag Chemie, Weinheim/Bergstrasse
33. Walker, N.A., Smith, F.A. 1975. Intracellular pH in *Chara corallina* measured by DMO distribution. *Plant Sci. Lett.* **4**:125